Journal of Biomolecular NMR (2025) 79:223–230
https://doi.org/10.1007/s10858-025-00469-8

ARTICLE

Estimating cross-relaxation rates between methyl and neighboring labile proton spins in high molecular weight proteins

Vitali Tugarinov[1] · **G. Marius Clore**[1]

Received: 6 February 2025 / Accepted: 6 May 2025 / Published online: 25 May 2025
This is a U.S. Government work and not under copyright protection in the US; foreign copyright protection may apply 2025

Abstract

We show that water saturation leads to deleterious losses in sensitivity of methyl signals in selectively methyl-[$^{13}CH_3$]-labeled protein samples of high molecular weight proteins dissolved in H_2O. These losses arise from efficient cross-relaxation between methyl protons and proximal labile protons in the protein structure. A phenomenological model for analysis of methyl intensity decay profiles that involves exchange saturation transfer of magnetization from localized proton spins of water to various labile groups in the protein structure that, in turn, efficiently cross-relax with protons of methyl groups, is described. Analysis of methyl intensity decay profiles with this model allows cross-relaxation rates (σ) between methyl and labile protons to be determined and permits identification of methyl sites in close proximity to labile groups in the protein structure.

Keywords Exchange saturation transfer · Cross relaxation · Hydrogen exchange · Methyl NMR of high-molecular-weight proteins · Water saturation

Methyl groups have played a special role in NMR studies of protein structure and side-chain dynamics yielding important insights into kinetics, thermodynamics and mechanisms of a large variety of biochemical processes (Tugarinov et al. 2004; Ruschak and Kay 2010; Rosenzweig and Kay 2014; Schütz and Sprangers 2020). Typically, NMR experiments targeting methyl groups of high molecular weight proteins are applied to protein samples that are selectively isotopically labeled with $^{13}CH_3$ methyl groups on a highly deuterated background (Tugarinov et al. 2006). Although for many NMR experiments that target methyl groups, the isotopically labeled protein samples may be prepared in D_2O solvent, oftentimes they are dissolved in H_2O as a matter of convenience – for example, if the same sample is planned to be used for NMR applications involving backbone ^1H-^{15}N amide groups. In addition, H_2O is ~ 20% less viscous than D_2O (Cho et al. 1999), resulting in a lower global rotational correlation time, τ_C, of the protein of interest. When selectively [$^{13}CH_3$]-methyl-labeled proteins are dissolved in H_2O, however, problems may arise with water suppression in heteronuclear multiple-quantum coherence (HMQC)-based NMR experiments (Mueller 1979; Bax et al. 1983; Tugarinov et al. 2003). As methyl hydrogens do not exchange with water, it may be tempting to achieve satisfactory water suppression by saturating the water signal with a weak radio-frequency (RF) field.

Here we demonstrate that water saturation leads to deleterious losses in sensitivity of methyl signals in selectively methyl-[$^{13}CH_3$]-labeled protein samples of high molecular weight proteins dissolved in H_2O. We show that even if water is saturated with a relatively weak RF field strength (< 50 Hz), the decrease in observed methyl signal intensities may be very substantial (up to a factor of 4) in high molecular weight proteins. These losses in sensitivity are traced to efficient cross-relaxation between methyl protons and the proximal labile protons in the protein structure that are in moderately fast exchange with (saturated) water. We describe a phenomenological model for analysis of methyl intensity decay profiles that involves exchange saturation transfer of magnetization from localized water proton spins to various labile groups in the protein that can, in turn, cross-relax efficiently with methyl protons. This model allows for the determination of cross-relaxation rates (σ) between methyl and labile proton spins and the identification of

✉ Vitali Tugarinov
vitali.tugarinov@nih.gov

✉ G. Marius Clore
mariusc@mail.nih.gov

[1] Laboratory of Chemical Physics, National Institute of Diabetes and Digestive and Kidney Diseases, National Institutes of Health, Bethesda, MD 20892-0520, USA

methyl sites in close proximity to one or more labile protons in the protein structure.

The detrimental effects of water saturation are demonstrated on the {U-[^{15}N,^{2}H]; Ileδ1-[^{13}CH$_3$]}-labeled sample of an 82-kDa enzyme Malate Synthase G (MSG) at 5 °C (τ_C ~ 90 ns) and 30 °C (τ_C ~ 45 ns) using the recently developed gradient-selected delayed decoupling ^{1}H-^{13}C HMQC experiments, dd-(^{1}H-^{13}C)-HMQC (Bolik-Coulon et al. 2023; Ahmed et al. 2024), immediately preceded by a 2.5 s-long water saturation period. Although the gradient selection of multiple-quantum ^{1}H-^{13}C coherences leads to a $\sqrt{2}$ loss of sensitivity compared to amplitude-modulated experiments, gradient selection is indispensible for ensuring high quality 2D (^{1}H-^{13}C)-HMQC correlation spectra irrespective of the strength of the water saturation field, B_1, employed. For Ileδ1 methyl groups of MSG, the gradient selected dd-(^{1}H-^{13}C)-HMQC experiment (Ahmed et al. 2024) provides sensitivity gains of 33 ± 15% and 12 ± 9% at 5 °C and 30 °C, respectively, compared to the same experiments without delayed decoupling.

Figure 1 shows the decay profiles of methyl peak intensities typically obtained for selectively [^{13}CH$_3$]-labeled and otherwise deuterated samples of ubiquitin at 5 °C (τ_C ~ 9 ns; shown in green), and MSG at 5 °C (τ_C ~ 90 ns; shown in red) and 30 °C (τ_C ~ 45 ns; shown in blue) as a function of the saturation field strength B_1. In all cases, the intensities are normalized to those obtained without water saturation ($B_1 = 0$). The profiles have a characteristic biphasic shape, with the steep decrease in signal intensity associated with the initial phase of the curve (up to B_1 ~ 25 Hz) clearly dependent on τ_C. As we show below, the extent of this initial drop in intensity is exquisitely sensitive to cross-relaxation rates (σ) between methyl protons and proximal labile hydrogens, but also depends on: (1) longitudinal relaxation rates (R_1) of both methyl and labile protons, and (2) the rate of exchange of labile hydrogens with water (k_{ex}). The second phase of each curve is characterized by a monotonic decay of signal intensity that is primarily determined by transverse relaxation rates (R_2) of both methyl and labile ^{1}H spins. We note that this monotonic decay may be contrasted to the genuine steady state reached in heteronuclear 'steady-state' NOE experiments for ^{1}H-^{15}N/^{1}H-^{13}C spin-systems, where the magnetization of a heteronucleus (^{15}N/^{13}C) is not directly perturbed by ^{1}H saturation.

The labile hydrogens in fast exchange may include non-hydrogen-bonded backbone amides (Wüthrich 1986; Grzesiek and Bax 1993); the amides of Asn and Gln side chains (Wüthrich 1986; Klein et al. 2019); hydroxyl groups of Ser, Thr and Tyr (Liepinsh et al. 1992; Takeda et al. 2011, 2009); Cys thiol groups (Takeda et al. 2010); guanidinium groups of Arg (Mackenzie and Hansen 2019); and amino groups of Lys side-chains (Iwahara et al. 2007). The abundance of labile ^{1}H spins with unknown relaxation properties, chemical shifts and hydrogen exchange rates in the vicinity of each methyl site, makes rigorous modeling of the intensity decay profiles impossible. Below we describe

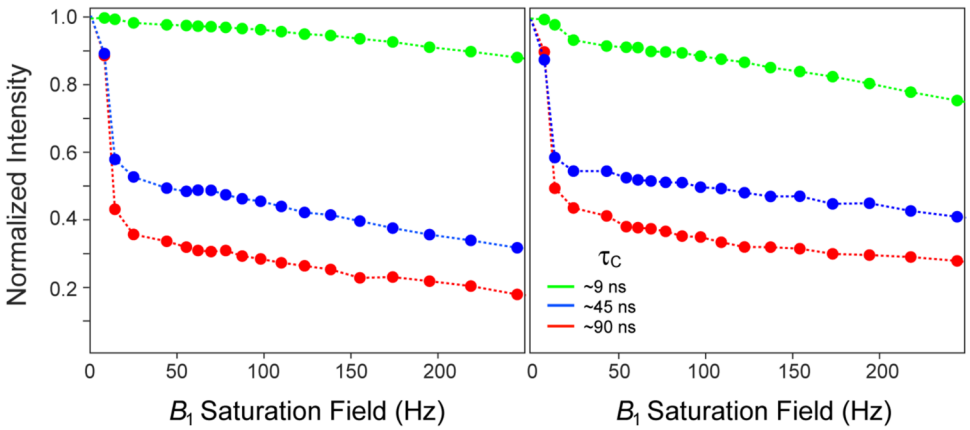


Fig. 1 Typical intensity decay curves obtained for selectively [^{13}CH$_3$]-labeled and otherwise deuterated protein samples with varying rotational correlation times, τ_C, as a function of the saturation field strength B_1. Examples are drawn from Leu^{67} δ2 (*left panel*) and Leu^{50} δ2 (*right panel*) methyl groups of the 7.5-kDa protein ubiquitin (green circles, τ_C ~ 9 ns), and Ile^{200} δ1 (*left panel*) and Ile^{260} δ1 (*right panel*) methyl groups of the 82-kDa Malate Synthase G (MSG) at 30 ºC (blue circles, τ_C ~ 45 ns) and 5 ºC (red circles, τ_C ~ 90 ns). The 0.5 mM sample of {U-[^{15}N, ^{2}H]; Ileδ1-[^{13}CH$_3$]}-labeled MSG was dissolved in a buffer containing 90% H_2O/ 10% D_2O (v/v), 20 mM sodium phosphate (pH 7.0), 5 mM $MgCl_2$ and 0.05% of NaN_3. The 1.3 mM {U-[^{15}N, ^{2}H]; Ileδ^{1}-[^{13}CH$_3$]; Leu,Val-[^{13}CH$_3$,^{12}CD$_3$]}-labeled sample of ubiquitin was dissolved in a buffer containing 90% H_2O/10% D_2O (v/v), 20 mM sodium phosphate (pH 7.0) and 50 mM NaCl. The data were obtained using either 2D gradient-selected dd-(^{1}H-^{13}C)-HMQC experiment (Ahmed et al. 2024) (for MSG) or a gradient-selected 2D (^{1}H-^{13}C)-HMQC (for ubiquitin) immediately preceded by a 2.5 s long ^{1}H continuous wave (CW) saturation at the frequency of the water signal. All data were recorded on a 600 MHz AVANCE HD Bruker spectrometer equipped with a triple-axis (*x*, *y*, *z*) gradient cryogenic probe. The connecting dashed lines do not represent best-fits and are shown merely to guide the eye

a phenomenological, semi-quantitative approach that was adopted for analysis of intensity decay profiles with the primary focus on determination of the cross-relaxation rates σ between methyl and labile ^{1}H spins. The minimalistic model that satisfies experimental intensity decay profiles, is comprised of three distinct sites: (1) methyl protons (labeled with 'M' superscripts), (2) labile protons (superscript 'H') that cross-relax with methyl protons and, at the same time, are involved in hydrogen exchange with (3) protons of 'localized' water molecules (superscript 'W'). The set of Bloch-McConnell equations (McConnell 1958; Helgstrand et al. 2000) describing the evolution of magnetization of this 3-site system is given by,

$$\frac{d}{dt}\begin{bmatrix} E \\ I_x^{\mathrm{M}} \\ I_y^{\mathrm{M}} \\ I_z^{\mathrm{M}} \\ I_x^{\mathrm{H}} \\ I_y^{\mathrm{H}} \\ I_z^{\mathrm{H}} \\ I_x^{\mathrm{W}} \\ I_y^{\mathrm{W}} \\ I_z^{\mathrm{W}} \end{bmatrix} = -\begin{bmatrix} 0 & 0 & 0 & 0 & 0 & 0 & 0 & 0 & 0 & 0 \\ 0 & R_2^{\mathrm{M}} & \Omega^{\mathrm{M}} & 0 & \sigma_R & 0 & 0 & 0 & 0 & 0 \\ 0 & -\Omega^{\mathrm{M}} & R_2^{\mathrm{M}} & \omega_1 & 0 & \sigma_R & 0 & 0 & 0 & 0 \\ \Theta^{\mathrm{M}} & 0 & -\omega_1 & R_1^{\mathrm{M}} & 0 & 0 & \sigma & 0 & 0 & 0 \\ 0 & \sigma_R/3 & 0 & 0 & R_2^{\mathrm{H}}+k_{ex}/2 & \Omega^{\mathrm{H}} & 0 & -k_{ex}/2 & 0 & 0 \\ 0 & 0 & \sigma_R/3 & 0 & -\Omega^{\mathrm{H}} & R_2^{\mathrm{H}}+k_{ex}/2 & \omega_1 & 0 & -k_{ex}/2 & 0 \\ \Theta^{\mathrm{H}} & 0 & 0 & \sigma/3 & 0 & -\omega_1 & R_1^{\mathrm{H}}+k_{ex}/2 & 0 & 0 & -k_{ex}/2 \\ 0 & 0 & 0 & 0 & 0 & 0 & 0 & R_2^{\mathrm{W}} & \Omega^{\mathrm{W}} & 0 \\ 0 & 0 & 0 & 0 & 0 & 0 & 0 & -\Omega^{\mathrm{W}} & R_2^{\mathrm{W}} & \omega_1 \\ \Theta^{\mathrm{W}} & 0 & 0 & 0 & 0 & 0 & 0 & 0 & -\omega_1 & R_1^{\mathrm{W}} \end{bmatrix}\begin{bmatrix} E \\ I_x^{\mathrm{M}} \\ I_y^{\mathrm{M}} \\ I_z^{\mathrm{M}} \\ I_x^{\mathrm{H}} \\ I_y^{\mathrm{H}} \\ I_z^{\mathrm{H}} \\ I_x^{\mathrm{W}} \\ I_y^{\mathrm{W}} \\ I_z^{\mathrm{W}} \end{bmatrix} \quad (1)$$

where I_j^{K} represents the deviation of the component $j \in \{x, y, z\}$ of the angular momentum of a nuclear spin for state $\mathrm{K} \in$ {'M'; 'H'; 'W'} from thermal equilibrium; R_1^{K} and R_2^{K} are longitudinal and transverse relaxation rates, respectively, of state K; Ω^{K} are frequency offsets of each state K from the frequency of the saturation field B_1; ω_1 is strength of the continuous-wave (CW) saturation field B_1 (applied along the x-axis; rad/s); σ is longitudinal cross-relaxation rate between methyl protons 'M' and the labile proton 'H'; σ_R is transverse cross-relaxation rate (ROE) between the sites 'M' and 'H', assumed, in the macromolecular limit, equal to, σ_R=-2σ; k_{ex} is a phenomenological rate constant that couples the evolution of labile protons with that of 'localized' water molecules (describing hydrogen exchange between protons 'H' and 'W'); $\Theta^{\mathrm{M}} = -R_1^{\mathrm{M}} - \sigma$; $\Theta^{\mathrm{H}} = -R_1^{\mathrm{H}} - \sigma/3$; $\Theta^{\mathrm{W}} = -R_1^{\mathrm{W}}$; E is unity; the initial conditions (at the start of the saturation period) are: $I_0 = [1\ 0\ 0\ 0\ 0\ 0\ 0\ 0\ 0\ 0\ 0\ 0\ 1]^T$, with '$T$' denoting transposition. Note that the rate of cross-relaxation of the three magnetically equivalent methyl protons 'M' with labile protons 'H' is threefold larger than that between ^{1}H spins in a ^{1}H-^{1}H spin-pair and, in the macromolecular limit, given by, $\sigma = -(3/10)\left(\mu_0/4\pi\right)^2(\gamma_H^4\hbar^2S^2\tau_C/r_{hh}^6)$, where γ_{H} is the gyromagnetic ratio of ^{1}H spins, μ_0, the vacuum permeability constant, r_{hh} is the $(<r^{-3}>)^{-1/3}$-averaged distance between methyl protons and protons 'H'; and S is the order parameter of the 'M'–'H' interaction.

The temporal changes in the value of I_z^{M}, calculated by integrating Eq. (1), were tracked as a function of the strength of the saturation field, ω_1, at several offsets from the water resonance frequency, Ω^{W}. The set of local (site-specific) variable parameters of the combined non-linear fit of intensity decays for all Ω^{W} comprised: {σ; k_{ex}; Ω^{H}}, while the rates R_1^{W} and R_2^{W} were used as global parameters (shared between all methyl sites). The transfer of magnetization from (saturated) water to labile proton spins via hydrogen exchange in the model of Eq. (1) is reminiscent of ^{1}H Chemical Exchange Saturation Transfer (CEST) experiments (Forsen and Hoffman 1963; Hoffman and Forsen 1966; Yuwen et al. 2017b, 2017a; Yuwen and Kay 2017)—particularly, their implementation for systems with *a-priori* known chemical shifts of the exchanging states (Ramanujam et al. 2019), with the important difference that methyl ^{1}H spins are coupled to the neighboring labile ^{1}H spins through dipolar cross-relaxation. As a consequence, the identification of proximal labile protons (Guivel-Scharen et al. 1998; Martinho et al. 2023) is indirect and based on the extracted values of cross-relaxation rates σ.

Hydrogen exchange of labile protons 'H' with water in the model of Eq. (1) involves water molecules that are spatially 'localized' (such as, for example, water molecules of the protein hydration shell in close proximity to labile protons (Van-Quynh et al. 2003; Bonechi et al. 2019) or those forming transient hydrogen bonds with the latter (Persson and Halle 2015)) as opposed to water molecules of the bulk solvent. If exchange with the bulk solvent is considered, the reaction of hydrogen exchange would obey the kinetic relationship, $k_{\mathrm{H}\to\mathrm{W}}[\mathrm{protein}] = k_{\mathrm{W}\to\mathrm{H}}[\mathrm{water}]$, where $k_{\mathrm{H}\to\mathrm{W}}$ and $k_{\mathrm{W}\to\mathrm{H}}$ are the first-order rate constants of the forward and backward exchange processes, respectively, and $k_{\mathrm{W}\to\mathrm{H}}$ would be downscaled by the ratio, [protein]/[water]. In that case, the magnetization of labile protons would essentially be un-coupled from the pool of solvent molecules. By contrast, if water molecules participating in hydrogen exchange are localized and distinguished from the bulk solvent, it may be assumed that $k_{\mathrm{H}\to\mathrm{W}} = k_{\mathrm{W}\to\mathrm{H}} = k_{ex}/2$, where $k_{ex} = k_{\mathrm{H}\to\mathrm{W}} + k_{\mathrm{W}\to\mathrm{H}}$. We note that the evolution of water

magnetization in the model of Eq. (1) does not depend on that of labile protons 'H' or k_{ex}, as we are not concerned with the 'fate' of water magnetization in the first place, while the localized water molecules are likely to be in very fast exchange with the bulk solvent—a process that is not included in the model. Also not included in the model are possible 'direct' dipolar interactions of methyl protons with bound (buried) water molecules (Otting 1997), or long-range dipolar couplings with the solvent (Halle 2003). Earlier studies showed that the residence time of water molecules buried in protein structures is on the order of several nanoseconds at the highest (G.M. Clore et al. 1990; G. M. Clore et al. 1994; Ernst et al. 1995; Otting 1997), and therefore such cross-relaxation is assumed to be negligible in the context of the present study. Likewise, cross-relaxation between methyl sites themselves is not accounted for in the model of Eq. (1), as methyl proton resonances are offset from the water saturation frequency by, $\Omega^M \sim -4$ ppm, and therefore inter-methyl cross-relaxation has only a minor impact on the second phase of methyl signal decay profiles (that is absorbed in the value of Ω^H in the fit).

The important advantage of the formulation in Eq. (1) consists in effective de-correlation of the rates σ and k_{ex}, permitting robust determination of σ for each methyl site from the set of intensity decays obtained at several offsets from the water frequency, Ω^W, largely irrespective of the assumptions about the relaxation rates of labile protons, R_1^H and R_2^H (which, as we describe below, can be fixed to uniform values to restrict the number of variable parameters of the fit). Figure 2 (*left panel*) shows that the sensitivity of the shape of the intensity decay profiles simulated using Eq. (1) to the value of k_{ex} is restricted to small exchange rates (up to a certain threshold of ~ 20 s^{-1}). On the other hand, although the rates σ may be strongly correlated to the offsets of labile protons from saturation frequency, Ω^H, the sensitivity of intensity decay shapes to Ω^H is quite low for the range of labile ^{1}H chemical shifts commonly encountered in proteins (Fig. 2, *right panel*). As a result, a very minor change in the value of σ can compensate for a major change in Ω^H. We note that the main limitation of the model in Eq. (1) derives from its reliance on the accurate values of longitudinal methyl ^{1}H relaxation rates, R_1^M, which have to be measured separately using the 'initial rate' approximation. Even partial break-down of the 'initial rate' approximation would compromise the accuracy of the extracted cross-relaxation rates. On another note, the scope of applicability of the model is constrained by the rates of hydrogen exchange between the water and labile proton spins (k_{ex})—the exchange rate slower than a certain threshold value leads to convex-shaped profiles (Fig. 2, *left panel*), irrespective of the value of σ. As a result, for slowly exchanging labile protons ($k_{ex} < \sim 1$ s), the cross-relaxation rates become indeterminable.

Methyl ^{1}H relaxation rates, R_2^M and the 'initial rate' approximation to R_1^M, were measured for each methyl site of MSG by straightforward extensions of gradient selected (^{1}H-^{13}C)-HMQC experiments (average values $< R_2^M > = 49$ s^{-1} and $< R_1^M > = 1.8$ s^{-1} were obtained for 37 Ileδ methyl groups of {U-[^{15}N, ^{2}H]; Ileδ1-[$^{13}CH_3$]}-labeled MSG at 5 °C; 600 MHz) and fixed in the non-linear best-fits of methyl normalized intensity profiles as a function of saturation field strength, ω_1, for three saturation frequency offsets from the water signal, -Ω^W: 0 (on-resonance saturation), -60 and − -200 Hz. Multiple fits were performed using {σ; k_{ex}; Ω^H} as methyl site-specific variable parameters, and

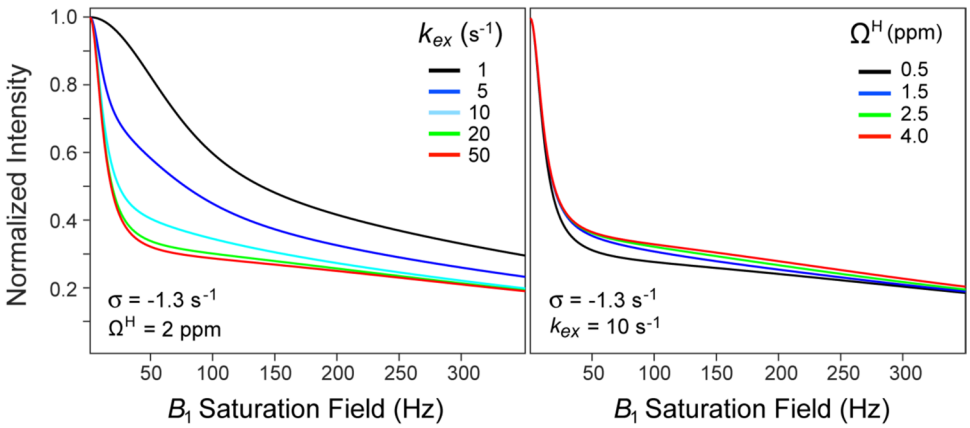


Fig. 2 Simulations showing the decay of normalized signal intensities as a function of the saturation B_1 field strength calculated using Eq. (1): (*Left panel*) for a range of k_{ex} values from 1 to 50 s^{-1}, with σ fixed at -1.3 s^{-1}, and $\Omega^H = 2$ ppm. (*Right panel*) for a range of Ω^H values from 0.5 to 4 ppm, with σ = -1.3 s^{-1} and $k_{ex} = 10$ s^{-1}. The B_1 field (ω_1) was applied at the frequency of water ($\Omega^W = 0$) for a duration of 2.5 s. All simulations were performed for a spectrometer frequency of 600 MHz using the following set of typical parameters for Ileδ1 methyl groups of MSG at 5 °C: $\Omega^M = -4.3$ ppm (from the carrier at 0); $R_1^M = 1.8$ s^{-1}; $R_2^M = 50$ s^{-1}; $R_1^H = 1.0$ s^{-1}; $R_2^H = 300$ s^{-1}; $R_1^W = 50$ s^{-1}; $R_2^W = 95$ s^{-1}; and $\sigma_R = -2$ σ = 2.6 s^{-1}

the rates $\{R_1^W;R_2^W\}$ as global variable parameters on a grid of fixed and uniform (the same for all methyl sites) values of $\{R_1^H;R_2^H\}$. Selected examples of such best-fit intensity decay profiles obtained for Ileδ1 sites of MSG at 5 °C (600 MHz), performed with R_1^H and R_2^H set to 0.8 s^{-1} and 300 s^{-1}, respectively, are shown in Fig. 3. Analysis of the results of such a grid-search showed that while the goodness-of-fit is very similar among individual minimizations, the best-fit σ values are remarkably robust to variations in $\{R_1^H;R_2^H\}$—in particular, the calculated maximal standard deviation of the mean $\sigma, <\sigma>$, is only 0.012 s^{-1} for a range of R_1^H rates between 0.6 and 2.4 s^{-1} and a range of R_2^H between 150 and 600 s^{-1}. We verified that the same applies to individual values of σ for each methyl site. The best-fit values of σ for Ileδ1 sites of MSG at 5 °C varied from -0.6 to -3.5 s^{-1} ($<\sigma> = -1.25 \pm 0.63$ s^{-1}).

In principle, the cross-relaxation rates σ may be determined from a single decay profile, with water saturated on-resonance, albeit at the expense of other parameters of the model remaining ill-determined (especially, the offsets of labile protons from saturation frequency, Ω^H). Recording of several decay profiles with different B_1 field offsets, significantly improves the precision of the extracted σ rates. The choice of B_1 field offsets is dictated by the steep dependence of the shape of decay profiles – particularly, the initial 'drop-off' of intensities – on the B_1 field offsets (Fig. 3). We observed that the best results are achieved when the B_1 field offsets, Ω^W, are approximately uniformly distributed in the range, $0 \le \Omega^W \le \sim 0.5\omega_{1,max}$, where $\omega_{1,max}$ is the largest B_1 field strength employed (typically, 350–400 Hz).

While the choice of R_2^H in the fits to the model in Eq. (1), affects primarily the fitted values of Ω^H (*i.e.* the errors/variations in R_2^H are absorbed mainly by Ω^H), the choice of R_1^H correlates and anti-correlates with the fitted k_{ex} and Ω^H values, respectively. As neither k_{ex} nor Ω^H can be meaningfully interpreted in the approximate model described by Eq. (1), we focus here exclusively on the cross-relaxation rate σ – the only parameter that is largely invariant to the choice of $\{R_1^H;R_2^H\}$. For reference, we note that in the fits where R_1^H and R_2^H are set to 0.8 s^{-1} and 300 s^{-1}, respectively, k_{ex} for individual methyl sites varied between 1 and 30 s^{-1} ($<k_{ex}> = 5.5 \pm 4.3$ s^{-1}), while the values of Ω^H varied from +0.3 to +3.0 ppm from the chemical shift of water ($<\Omega^H> = +1.8 \pm 0.6$ ppm from water). The optimized values of the rates R_1^W and R_2^W were 49.7 ± 1.2 s^{-1} and 95.6 ± 2.1 s^{-1}, respectively, and report on the inhomogeneity of the applied B_1 saturation field rather than the intrinsic relaxation rates of water ^{1}H spins.

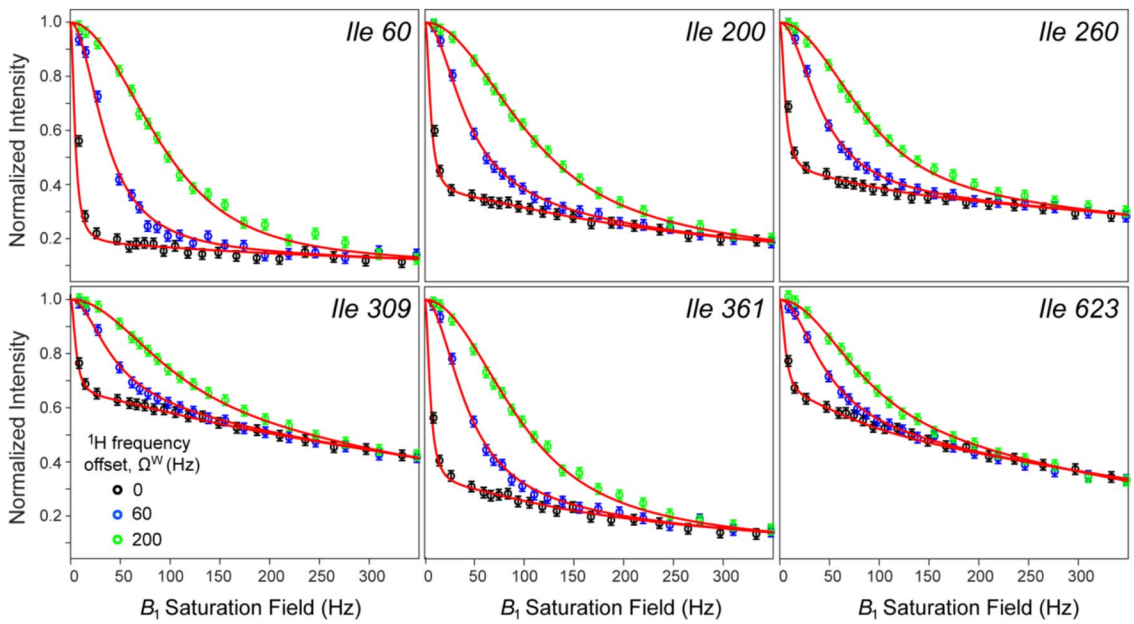


Fig. 3 Selected examples of 2D cross-peak intensity decay curves obtained for the {U-[^{15}N, ^{2}H]; Ileδ1-[$^{13}CH_3$]}-labeled sample of MSG at 5 °C ($\tau_C \sim 90$ ns) as a function of the saturation field strength, ω_1. The data were obtained with the 2D dd-(^{1}H-^{13}C)-HMQC experiment preceded by a ^{1}H CW saturation period with a duration of 2.5 s at or near the frequency of the water signal. The experimental data obtained with the ^{1}H saturation performed on-resonance with the water signal are represented by open black circles, while the data obtained with ^{1}H saturation frequency offset up-field of the water resonance by 60 and 200 Hz, are shown with blue and green open circles, respectively. The values fitted to the model in Eq. (1) at each frequency offset are shown with red solid curves. The fits were performed as described in the text using fixed and uniform values of $R_1^H = 0.8$ s^{-1} and $R_2^H = 300$ s^{-1}. The data were acquired at 600 MHz; sample conditions are listed in Fig. 1

Figure 4A compares the values of σ obtained at 5 (black bars) and 30 °C (red bars). Although on average the values of |σ| scale approximately proportionately to the global tumbling times ($<\sigma_{5C}> = -1.25\ s^{-1}$ versus $<\sigma_{30C}> = -0.69\ s^{-1}$), several methyl sites show very similar σ rates at 5 and 30 °C (*e.g.* Ile[12], Ile[42]; Fig. 4A) possibly reflecting different contributions of local side-chain motions at the two temperatures. To gain more confidence in the obtained cross-relaxation rates σ, we performed the measurements of methyl intensity decay profiles for Ileδ1 sites of MSG at 900 MHz (5 °C), and analyzed the data in the same manner with the model in Eq. (1). The correlation plot comparing the values of σ obtained at 600 and 900 MHz spectrometer fields (both at 5 °C) is shown in Fig. 4B. The values of σ at 900 MHz (σ_{900}; *y*-axis) are consistently smaller by absolute magnitude (by 9% on average) than their counterparts obtained at 600 MHz (σ_{600}; *x*-axis). This difference is much larger than the calculated contribution of the spectral density at $2\omega_H$ frequency, $J(2\omega_H)$, to σ for a molecule with a $\tau_C = 90$ ns if only global molecular motion is considered, and may likewise reflect the role played by local motions in the interactions between methyl and labile proton spins.

The largest values of |σ| obtained at either of the two or both temperatures (5 and 30 °C; Fig. 4A) are associated with Ile δ1 methyl sites that are located in close proximity to one or more labile, non-hydrogen-bonded protons in the three-dimensional structure of MSG (Howard et al. 2000) (pdb access code 1d8c). The distances to the nearest (located at ≤ 4.5 Å) labile, non-hydrogen-bonded protons in the structure of MSG for 6 methyl Ile δ1 sites with the largest |σ| rates (Fig. 4A) are summarized in Table 1. The shortest distance between methyl protons and the labile proton spin 'H', r_{hh} (estimated from the largest |σ| assuming the order parameter of the interaction $S^2 = 1$, and $\tau_C = 90$ ns for MSG at 5 °C, from the relationship, $\sigma = -(3/10)\left(\mu_0/4\pi\right)^2(\gamma_H^4\hbar^2S^2\tau_C/r_{hh}^6)$is 4.0 Å, while the longest distance is 5.4 Å. We note that as the order parameters for methyl-side-chain (methyl ^{1}H – labile ^{1}H) interactions in a protein are quite unlikely to be close to unity, these values almost certainly represent upper bounds on inter-proton distances. It is also worth noting that the interpretation of the smallest cross-relaxation rates |σ| in terms of distances to neighboring labile ^{1}H spins is prone to errors because labile protons whose exchange rates with water (k_{ex}) are slowed down (e.g. due to inaccessibility to the solvent or hydrogen-bonding), may be present in close proximity to a given methyl Ileδ1 site. The proximity of such relatively slowly-exchanging labile protons to a given methyl site, however, will result in convex-shaped profiles (see Fig. 2, *left panel*) and will not be captured by the model in Eq. (1). Nevertheless, among 5 Ileδ1 methyl sites of MSG with the lowest |σ| rates, only one (Ile[5]) has a labile, non-hydrogen-bonded side-chain proton located at a distance of less than 5 Å ($H^{\zeta 3}$ of Lys[17] at 4.4 Å).

The application of pulsed field gradients to achieve quadrature detection in the indirect dimension of dd-(^{1}H-^{13}C)-HMQC experiments (Ahmed et al. 2024) used in this work, leads to a $\sqrt{2}$ loss in sensitivity compared to their amplitude-modulated analogues. For Ileδ1 methyl sites of MSG at 5 ºC, the major portion of this loss is recovered by the use of delayed decoupling. For methyl-labeled protein

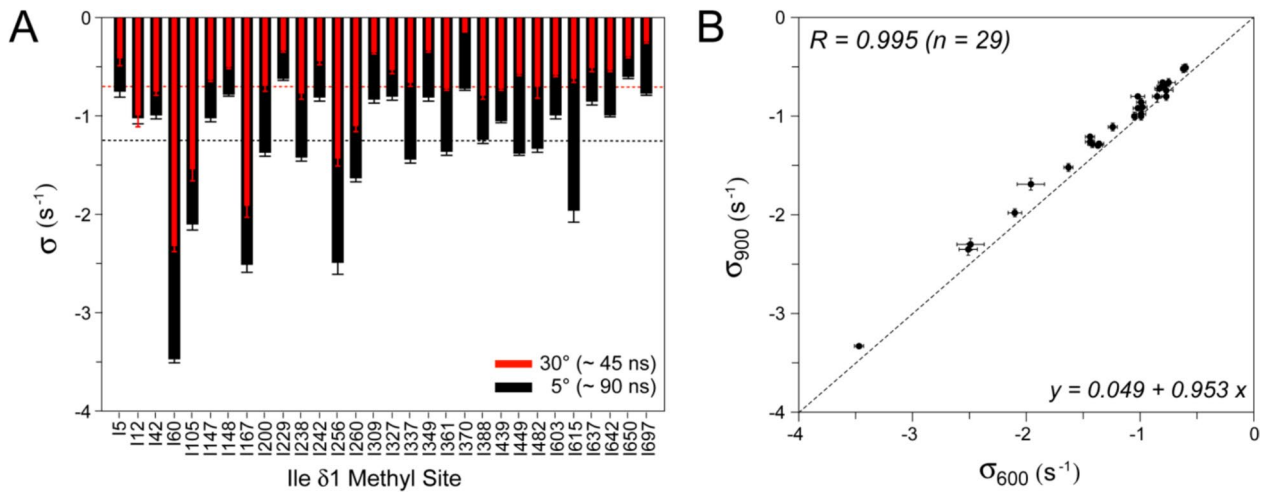


Fig. 4 Comparison of σ values extracted for Ile δ1 methyl groups of {U-[^{15}N, ^{2}H]; Ile δ1-[$^{13}CH_3$]}-MSG using the model in Eq. (1) under different experimental conditions. **A** Plot comparing σ values obtained at 5 °C (wide black bars; $\tau_C \sim 90$ ns) and 30 °C (narrow red bars; $\tau_C \sim 45$ ns). Horizontal dashed lines correspond to the mean of all obtained σ values for each dataset. Both datasets were obtained at 600 MHz. **B** Correlation plot of σ values obtained at 600 MHz (*x*-axis) and 900 MHz (*y*-axis); both datasets were obtained at 5 °C. The parameters of linear regression for $n = 29$ methyl sites are shown on the plot. The diagonal dashed line corresponds to $y = x$

Table 1 Distances to the nearest (≤4.5 Å) labile, non-hydrogen-bonded protons for methyl Ile δ1 sites of MSG (Howard et al. 2000) with the largest |σ| rates

Ile δ1 Site	Labile ^{1}H	Distance (Å)
Ile^{60}	Arg^{430} guanidinium:	
	$H^{\eta 2(b)}$	2.9$^{(b)}$
	$H^{\eta 1(b)}$	3.1$^{(b)}$
	H^{ε}	3.2
Ile^{105}	Ser^{384} hydroxyl:	
	H^{γ}	2.7
	Thr^{102} hydroxyl:	
	H^{γ}	2.9
	Tyr^{387} hydroxyl:	
	H^{η}	2.9
	Lys^{421} (NH_3^+)$^{(c)}$	
	H^{ζ}	4.0–4.5$^{(c)}$
Ile^{167}	Tyr^{139} hydroxyl:	
	H^{η}	2.6
	Arg^{171} guanidinium:	
	$H^{\eta 1(b)}$	4.1$^{(b)}$
Ile^{256}	Tyr^{139} hydroxyl:	
	H^{η}	4.0
	Arg^{171} guanidinium:	
	$H^{\eta 1(b)}$	2.9$^{(b)}$
	$H^{\eta 2(b)}$	2.8$^{(b)}$
Ile^{260}	Ser^{137} hydroxyl:	
	H^{γ}	4.0
	Ser^{137} backbone:	
	H^{N}	4.3
	Arg^{317} guanidinium:	
	$H^{\eta 2(b)}$	4.3$^{(b)}$
Ile^{615}	Ser^{618} hydroxyl:	
	H^{γ}	4.0

The distances calculated for each proton of a methyl group were $(< r^{-6} >)^{-1/6}$-averaged. $^{(b)}$The shortest of the distances to the two η protons of guanidinium groups is indicated. $^{(c)}$The range of distances to the three ζ protons of NH_3^+ groups is specified

samples dissolved in H_2O where the loss of a $\sqrt{2}$ is prohibitive, suppression of the water signal may be achieved by application of selective water pulses or selective excitation of methyl protons as developed for SOFAST-methyl-TROSY spectroscopy (Amero et al. 2009). Both these methods may be combined with the delayed decoupling scheme (Bolik-Coulon et al. 2023).

In summary, we show that deleterious decreases in methyl signal intensities are observed in selectively methyl-labeled protein samples of high-molecular-weight proteins dissolved in H_2O, when water is saturated. These losses in sensitivity are traced to efficient cross-relaxation between methyl protons and proximal labile proton spins in the protein structure that are in fast exchange with (saturated) water. A phenomenological model describing exchange saturation transfer of magnetization from localized proton spins of water to labile groups in the protein structure that, in turn, efficiently cross-relax with methyl protons, allows for determination of cross-relaxation rates (σ) between methyl and labile protons and permits identification of methyl sites in close proximity to one or more labile groups in the protein structure.

Acknowledgement We thank Drs. Dennis Torchia, Jinfa Ying and Juan Lopez-Smith (NIDDK, NIH) for useful suggestions, Dr. Francesco Torricella for preparing NMR samples, and Drs. James Baber and Dan Garrett (NIDDK, NIH) for technical support. We are grateful to Prof. Lewis E. Kay (University of Toronto) for providing the Bruker pulse code and software for processing of dd-HMQC data. This work was supported by the Intramural Program of the National Institute of Diabetes and Digestive and Kidney Diseases, National Institutes of Health (DK029023 to G.M.C.).

Author contributions V.T. collected and analyzed the data; V.T. and G.M.C. wrote the paper.

Funding Open access funding provided by the National Institutes of Health. National Institute of Diabetes and Digestive and Kidney Diseases, DK029023, DK029023.

Data availability No datasets were generated or analysed during the current study.

Declarations

Conflict of interest The authors have no competing interests to declare that are relevant to the content of this article.

Open Access This article is licensed under a Creative Commons Attribution 4.0 International License, which permits use, sharing, adaptation, distribution and reproduction in any medium or format, as long as you give appropriate credit to the original author(s) and the source, provide a link to the Creative Commons licence, and indicate if changes were made. The images or other third party material in this article are included in the article's Creative Commons licence, unless indicated otherwise in a credit line to the material. If material is not included in the article's Creative Commons licence and your intended use is not permitted by statutory regulation or exceeds the permitted use, you will need to obtain permission directly from the copyright holder. To view a copy of this licence, visit http://creativecommons.org/licenses/by/4.0/.

References

Ahmed R, Rangadurai AK, Ruetz L, Tollinger M, Kreutz C, Kay LE (2024) A delayed decoupling methyl-TROSY pulse sequence for atomic resolution studies of folded proteins and RNAs in condensates. J Magn Reson 362:107667

Amero C, Schanda P, Dura MA, Ayala I, Marion D, Franzetti B, Brutscher B, Boisbouvier J (2009) Fast two-dimensional NMR spectroscopy of high molecular weight protein assemblies. J Am Chem Soc 131:3448–3449

Bax A, Griffey RH, Hawkings BL (1983) Correlation of proton and nitrogen-15 chemical shifts by multiple quantum NMR. J Magn Reson 55:301–315

Bolik-Coulon N, Sever AIM, Harkness RW, Aramini JM, Toyama Y, Hansen DF, Kay LE (2023) Less is more: a simple methyl-TROSY based pulse scheme offers improved sensitivity in applications to high molecular weight complexes. J Magn Reson 346:107326

Bonechi C, Tamasi G, Pardini A, Donati A, Volpi V, Leone G, Consumi M, Magnani A, Rossi C (2019) Ordering effect of protein surfaces on water dynamics: NMR relaxation study. Biophys Chem 249:106149

Cho CH, Urquidi J, Singh S, Robinson GW (1999) H_2O and D_2O viscosity. J Phys Chem B 103:1991–1994

Clore GM, Bax A, Wingfield PT, Gronenborn AM (1990) Identification and localization of bound internal water in the solution structure of interleukin 1b by heteronuclear three-dimensional ^{1}H rotating-frame overhauser ^{15}N–^{1}H multiple quantum coherence NMR spectroscopy. Biochemistry 29:5671–5676

Clore GM, Bax A, Omichinski JG, Gronenborn AM (1994) Localization of bound water in the solution structure of a complex of the erythroid transcription factor GATA-1 with DNA. Structure 2:89–94

Ernst JA, Clubb RT, Zhou HX, Gronenborn AM, Clore GM (1995) Demonstration of positionally disordered water within a protein hydrophobic cavity by NMR. Science 267:1813–1817

Forsen S, Hoffman RA (1963) Study of moderately rapid chemical exchange reactions by means of nuclear magnetic double resonance. J Chem Phys 39:2892–2901

Grzesiek S, Bax A (1993) Measurement of amide proton exchange rates and NOEs with water in ^{13}C/^{15}N-enriched calcineurin b. J Biomol NMR 3:627–638

Guivel-Scharen V, Sinnwell T, Wolff SD, Balaban RS (1998) Detection of proton chemical exchange between metabolites and water in biological tissues. J Magn Reson 133:36–45

Halle B (2003) Cross-relaxation between macromolecular and solvent spins: the role of long-range dipole couplings. J Chem Phys 119:12372–12385

Helgstrand M, Hard T, Allard P (2000) Simulations of NMR pulse sequences during equilibrium and non-equilibrium chemical exchange. J Biomol NMR 18:49–63

Hoffman RA, Forsen S (1966) Transient and steady state overhauser experiments in the investigation of relaxation processes; analogies between chemical exchange and relaxation. J Chem Phys 45:2049–2060

Howard BR, Endrizzi JA, Remington SJ (2000) Crystal structure of *Escherichia Coli* malate synthase G complexed with magnesium and glyoxylate at 2.0 a resolution: mechanistic implications. Biochemistry 39:3156–3168

Iwahara J, Jung YS, Clore GM (2007) Heteronuclear NMR spectroscopy for lysine NH_3 groups in proteins: unique effect of water exchange on ^{15}N transverse relaxation. J Am Chem Soc 129:2971–2980

Klein SA, Majumdar A, Barrick D (2019) A second backbone: The contribution of a buried asparagine ladder to the global and local stability of a leucine-rich repeat protein. Biochemistry 58:3480–3493

Liepinsh E, Otting G, Wuthrich K (1992) NMR spectroscopy of hydroxyl protons in aqueous solutions of peptides and proteins. J Biomol NMR 2:447–465

Mackenzie HW, Hansen DF (2019) Arginine side-chain hydrogen exchange: quantifying arginine side-chain interactions in solution. ChemPhysChem 20:252–259

Martinho RP, Olsen GL, Frydman L (2023) CEST-based detection of labile protons by ultrafast 2D NMR. J Magn Reson Open 14–15:100096

McConnell HM (1958) Reaction rates by nuclear magnetic resonance. J Chem Phys 28:430–431

Mueller L (1979) Sensitivity enhanced detection of weak nuclei using heteronuclear multiple quantum coherence. J Am Chem Soc 101:4481–4484

Otting G (1997) NMR studies of water bound to biological molecules. Prog Nucl Magn Reson Spectrosc 31:259–285

Persson F, Halle B (2015) How amide hydrogens exchange in native proteins. Proc Natl Acad Sci USA 112:10383–10388

Ramanujam V, Charlier C, Bax A (2019) Observation and kinetic characterization of transient Schiff base intermediates by CEST NMR spectroscopy. Angew Chem Int Ed Engl 58:15309–15312

Rosenzweig R, Kay LE (2014) Bringing dynamic molecular machines into focus by methyl-TROSY NMR. Annu Rev Biochem 83:291–315

Ruschak AM, Kay LE (2010) Methyl groups as probes of supra-molecular structure, dynamics and function. J Biomol NMR 46:75–87

Schütz S, Sprangers R (2020) Methyl TROSY spectroscopy: a versatile NMR approach to study challenging biological systems. Prog Nucl Magn Reson Spectrosc 116:56–84

Takeda M, Jee J, Ono AM, Terauchi T, Kainosho M (2009) Hydrogen exchange rate of tyrosine hydroxyl groups in proteins as studied by the deuterium isotope effect on Cζ chemical shifts. J Am Chem Soc 131:18556–18562

Takeda M, Jee J, Terauchi T, Kainosho M (2010) Detection of the sulfhydryl groups in proteins with slow hydrogen exchange rates and determination of their proton/deuteron fractionation factors using the deuterium-induced effects on the $^{13}C\beta$ NMR signals. J Am Chem Soc 132:6254–6260

Takeda M, Jee J, Ono AM, Terauchi T, Kainosho M (2011) Hydrogen exchange study on the hydroxyl groups of serine and threonine residues in proteins and structure refinement using NOE restraints with polar side-chain groups. J Am Chem Soc 133:17420–17427

Tugarinov V, Hwang PM, Ollerenshaw JE, Kay LE (2003) Cross-correlated relaxation enhanced ^{1}H–^{13}C NMR spectroscopy of methyl groups in very high molecular weight proteins and protein complexes. J Am Chem Soc 125:10420–10428

Tugarinov V, Hwang PM, Kay LE (2004) Nuclear magnetic resonance spectroscopy of high-molecular-weight proteins. Annu Rev Biochem 73:107–146

Tugarinov V, Kanelis V, Kay LE (2006) Isotope labeling strategies for the study of high-molecular-weight proteins by solution NMR spectroscopy. Nat Protoc 1:749–754

Van-Quynh A, Willson S, Bryant RG (2003) Protein reorientation and bound water molecules measured by ^{1}H magnetic spin-lattice relaxation. Biophys J 84:558–563

Wüthrich K (1986) NMR of proteins and nucleic acids. Wiley, New York

Yuwen T, Kay LE (2017) Longitudinal relaxation optimized amide ^{1}H-CEST experiments for studying slow chemical exchange processes in fully protonated proteins. J Biomol NMR 67:295–307

Yuwen T, Huang R, Kay LE (2017a) Probing slow timescale dynamics in proteins using methyl ^{1}H-CEST. J Biomol NMR 68:215–224

Yuwen T, Sekhar A, Kay LE (2017b) Separating dipolar and chemical exchange magnetization transfer processes in ^{1}H-CEST. Angew Chem Int Ed Engl 56:6122–6125

Publisher's Note Springer Nature remains neutral with regard to jurisdictional claims in published maps and institutional affiliations.